



Characterization of sites of different thermodynamic affinities on the same metal center via isothermal titration calorimetry

Eric G. Moschetta, Kristina M. Gans, Robert M. Rioux*

Department of Chemical Engineering, 165 Fenske Laboratory, The Pennsylvania State University, University Park, PA 16802, United States

ARTICLE INFO

Article history:

Received 4 December 2012

Revised 14 February 2013

Accepted 25 February 2013

Keywords:

Palladium

Phosphorus ligands

Calorimetry

Thermodynamics

Homogeneous catalysis

Solvent effects

ABSTRACT

We investigate the binding thermodynamics of a series of phosphorus ligands to a model compound, $\text{PdCl}_2(\text{solv})_2$, where solv refers to a molecule of solvent, using isothermal titration calorimetry (ITC). ITC allows for the quantification of the equilibrium binding constant, the binding enthalpy, and the binding stoichiometry all in a single experiment. For systems in which two equivalents of ligand were able to bind to the Pd center, the binding sites on each Pd center in solution showed a different thermodynamic affinity for the same ligand. Changes in binding modes between different phosphorus ligands were due to steric bulk and poor electron-donating ability of such ligands. Our results demonstrate ligand binding was strongly enthalpy-driven due to solvent reorganization, which is the rearrangement of solvent molecules in the bulk solvent and the solvent molecules surrounding the solvated species.

© 2013 Elsevier Inc. All rights reserved.

1. Introduction

The most important factors when considering the activity and selectivity of a homogeneous catalyst are how electronic and steric effects of ligands affect the coordination and electronic characteristics of the metal center. As such, the choice of ligands greatly impacts the types of reactions for which the catalyst is best suited. Phosphorus ligands are ubiquitous in organometallic chemistry and are studied extensively to relate ligand properties to catalytic activities and selectivities [1–3]. Experimental data, such as enthalpies of reaction, rate and equilibrium constants, and spectroscopic data, are frequently correlated with the electronic and steric properties of phosphorus ligands in order to predict trends in reactivity for other phosphorus ligands. Perhaps the most famous and useful parameters for describing phosphorus ligands are the Tolman cone angle (θ) and the Tolman electronic parameter (TEP, ν_{CO}). The cone angle is an empirical measure of the overall steric bulk of a phosphorus ligand while the TEP is an empirical measure of the ability of a phosphorus ligand to donate electrons to a metal [1]. Models such as QALE [4] (Quantitative Analysis of Ligand Effects) and ECW [5] (named for the *E*, *C*, and *W* parameters in the model itself) emphasize the σ - and π -acidities and basicities as well as the steric bulk of the tested ligands such that the inherent properties of the ligands may be used to understand trends in kinetics and thermodynamics of organometallic processes (i.e., a structure–function

relationship). The main issue with these parameters is that correlations between the observed kinetic and thermodynamic data and the ligand properties themselves are indirect. It would be more informative to measure the interactions between metal centers and ligands in solution directly such that contributions from other factors, namely the solvent, may be considered in the metal–ligand binding equilibria. Solvent is often implicated in catalytic mechanisms due to the fact that solvent molecules interact with metal centers and ligands in solution, but its exact role in a given mechanism is usually unknown and merely implied [6,7].

Pd chemistry is an integral part of homogeneous catalysis, particularly for cross-coupling reactions. C–C bond formation is an overwhelmingly popular synthetic technique, as evidenced by the development of such Pd chemistries as the Heck reaction [8], Suzuki coupling [9], and Sonogashira coupling [10]. These chemistries, particularly the Heck reaction, rely on the *in situ* generation of Pd(0) species from starting Pd salts, such as palladium acetate, $\text{Pd}(\text{OAc})_2$, and PdCl_2 . These Pd(II) species are reduced to Pd(0), the active species, most commonly by means of exogenous phosphine ligands added to the reaction mixture. The ligands bind to the Pd centers in order to form the active species. The thermodynamic stability that the ligands impart to the Pd(0) species is instrumental in determining the activity and selectivity of the organometallic complex. PdCl_2 is an easily accessible starting material and is used in cross-coupling reactions as an alternative to $\text{Pd}(\text{OAc})_2$. Pd(II) species such as PdCl_2 have special use in oxidation reactions, such as the famous Wacker process (oxidation of ethylene to acetaldehyde) for which Pd(0) species are often

* Corresponding author. Fax: +1 814 865 7846.

E-mail address: rioux@enr.psu.edu (R.M. Rioux).

Table 1

Cone angle (θ) and Tolman electronic parameter (TEP) data for the phosphorus ligands used in this study. There is no reported value for the TEP for PFu₃ in the literature. All other values are taken from Ref. [1].

Phosphine	Abbreviation	Cone angle, θ (degrees)	TEP, ν_{CO} (cm ⁻¹)
P(C ₆ H ₅) ₃	PPh ₃	145	2068.9
P(<i>p</i> -FC ₆ H ₅) ₃	P(<i>p</i> -FC ₆ H ₅) ₃	145	2071.3
P(C ₄ H ₉ O) ₃	PFu ₃	133	–
P(OC ₆ H ₅) ₃	P(OPh) ₃	128	2085.3
P(<i>o</i> -CH ₃ C ₆ H ₄) ₃	P(<i>o</i> -tolyl) ₃	194	2066.6

unsuitable [11,12]. Specifically, Pd(II) is a better reagent for oxidation reactions with substituted and cyclic olefins and alkynes, though catalytic processes involving Pd(II) frequently generate Pd(0) intermediates, which necessitates the use of a reoxidizing agent [13,14]. Thus, there is considerable interest in understanding the thermodynamic stability, and potential regeneration, of Pd species in homogeneous catalytic processes.

Calorimetry is an excellent medium for ascertaining data with respect to understanding catalytic activity and metal–ligand binding equilibria from a thermodynamic perspective. Obtaining thermodynamic data in the liquid phase for a variety of metal–ligand interactions allows organometallic chemists to design new chemical syntheses because the data reveal vital information regarding the stability of the resulting organometallic complexes and how the sterics and electronics of the metal center may influence the reaction pathway for a particular class of substrates [15]. Isothermal titration calorimetry (ITC) is a technique capable of characterizing receptor–ligand interactions in solvated systems, to measure the equilibrium binding constants, enthalpies of reaction, and reaction stoichiometries in a single experiment [16]. Briefly, ITC experiments consist of a sample cell containing a solution of the receptor (in our case, this is the metal complex PdCl₂(solvent)₂) and reference cell containing the solvent that are held at the same temperature. The titrant solution, a solution of ligand, is then titrated into the sample cell once the power rating supplied to the sample cell is constant (note: the power rating is the thermal compensation of the calorimeter that is applied to the sample cell to keep it at the same temperature as the reference cell). Heat is then evolved or absorbed due to the metal–ligand binding and the controller compensates for these heat effects to maintain the cell at a constant temperature. Ligand is injected into the cell until the system is saturated, that is, no additional heat is evolved or absorbed due to ligand binding, only heat of mixing is present, and the resulting peaks are integrated to determine the total amount of heat released per injection. These integrated heats are then fit to an appropriate binding model in order to obtain the equilibrium binding constant, enthalpy of reaction, and reaction stoichiometry. ITC is widely used in biological and supramolecular systems because the thermodynamic information reveals how the guests (ligands) interact with the hosts (receptors) such that optimal ligands and receptors may be designed for specific processes. Modern calorimeters are capable of measuring equilibrium constants as high as 10⁹ M⁻¹ due to their nW level of sensitivity [17]. This information is critical in any field where molecular recognition is a central topic, such as drug design, metalloenzymes, and protein–ligand interactions, among others, in which the objective is to maximize a host's affinity for a specific guest. There are extensive reviews of the ITC literature over the last decade, including how ITC is used to obtain kinetic data via heat evolution as well as new types of systems, such as zeolites and nanoparticles, that are being investigated calorimetrically [18–25].

This study aims to determine the thermodynamics of ligand binding to a model compound, PdCl₂(MeCN)₂ (1), in acetonitrile (MeCN) using various phosphorus ligands (see Table 1 in Section 3.1

for ligand properties) and to determine the effect of solvent on the thermodynamics of binding triphenylphosphine, PPh₃, to PdCl₂(solvent)₂ (2), where solvent is a molecule of solvent. We use ITC to characterize the metal–ligand interactions for each solvated system and discuss our results in terms of the known electronic and steric properties of the ligands and the inherent properties of the solvents. We supplement our calorimetric analysis with ³¹P NMR characterization of the reaction intermediates and products and UV–Vis spectroscopy to verify reaction stoichiometry, so that we may adequately describe the binding equilibria occurring in the ITC and validate the appropriate choice of binding model. Furthermore, we consider the solvation and desolvation of the solutes (1, 2, and the phosphorus ligands) and solvent reorganization manifesting themselves in metal–ligand binding equilibria.

2. ITC theory

ITC theory is well-developed in the literature, but due to the fact that there are very few studies of solution-phase calorimetry that attempt to discern different binding modes between metals and ligands in organometallic chemistry using thermodynamic data, we briefly introduce the main concepts behind ITC theory and emphasize the mathematics that are the most pertinent to our work. First, we consider the binding of a single type of ligand, L, with a metal receptor, M, in solution:



where n represents the total number of ligands (i.e., the binding stoichiometry) that bind to the metal and ML_n is the final complex that forms between the metal and n ligands. In our systems, M represents PdCl₂(solvent)₂ and L represents the series of phosphorus ligands. We will only consider two types of binding within the scope of this work, though interested readers are referred elsewhere for additional information with respect to the establishment of different binding models as well as full derivations of these models [26,27]. The first type of binding is independent binding, in which the metal may have several binding sites, but each site is thermodynamically identical and has the same thermodynamic affinity for the ligand. We can write the general equilibrium binding constant, K_i , for each binding step as

$$K_i = \frac{[ML_i]}{[ML_{i-1}][L]} \quad (2)$$

where the terms in brackets represent concentrations of the respective species, ML_i represents a metal center with i ligands bound to it, and ML_{i-1} represents a metal center with $i - 1$ ligands bound to it, extending from $i = 0$ to $i = n$. The second type of binding is multiple-site binding, in which the metal has two thermodynamically different types of sites. Specifically, each site has its own affinity for the same ligand, but the occupancy of one site does not affect the affinity of the other, that is, the sites do not exhibit cooperative binding behavior [26]. For our systems, we can model this behavior by considering the sequential binding of the same type of ligand to the same metal center twice ($n = 2$):



For Eqs. (3) and (4), the equilibrium constants are given by Eqs. (5) and (6), respectively

$$K_1 = \frac{[ML]}{[M][L]} \quad (5)$$

$$K_2 = \frac{[ML_2]}{[ML][L]} \quad (6)$$

With full expressions for the respective equilibrium constants, it is now possible to combine these expressions with mass balances on each component:

$$[M]_T = [M] + [ML] + [ML_2] \quad (7)$$

$$[L]_T = [L] + [ML] + 2[ML_2] \quad (8)$$

Eqs. (7) and (8) can be extended to any binding system of n ligands, noting that $[M]_T$ and $[L]_T$ are the *total* concentrations of metal and ligand in the calorimeter cell. These mass balances can be substituted into the expressions for the equilibrium constants, such that only the total concentrations (i.e., measurable quantities) appear in the final ITC equations. This flexibility allows the experimenter to track the progress of the binding equilibria by calculating the molar ratio, the total amount of ligand in the calorimeter cell to the total amount of metal in the cell, as the independent variable. The dependent variable in ITC experiments is the total amount of heat released per injection of ligand, dQ :

$$dQ = V \sum_i \Delta H_i d[ML_i] \quad (9)$$

where V is the volume of the calorimeter cell, ΔH_i is the enthalpy of binding for the formation of ML_i , and $d[ML_i]$ is the incremental amount of complex, ML_i , formed during the injection. Eq. (9) may be extended to any number of complexes in solution. Substituting Eqs. (5)–(8) into Eq. (9) allow dQ to be written explicitly in terms of K_i , ΔH_i , $[M]_T$, and $[L]_T$, meaning that the heats from each injection can be fit to a statistical model as a function of the molar ratio that determines the binding parameters (K_i , ΔH_i , and n_i) in a single experiment (see Supporting Information for the full equations and discussion).

3. Experimental

3.1. Materials and solution preparations

$PdCl_2$ and the phosphorus ligands $P(o\text{-tolyl})_3$, PFu_3 , and $P(p\text{-FC}_6\text{H}_4)_3$ were obtained from Alfa Aesar. $P(OPh)_3$ was obtained from TCI and PPh_3 was obtained from Sigma. MeCN and pyridine were obtained from EMD while DMSO was obtained from BDH and DMF was obtained from Sigma. All chemicals were used without further purification.

All 1–5 mM solutions of $PdCl_2(\text{solvent})_2$ were prepared by dissolving 8.9–44.3 mg of anhydrous $PdCl_2$ in 50 mL of the appropriate degassed solvent and stirred vigorously overnight with gentle heating. The structures of $PdCl_2(\text{solvent})_2$ for each solvent are *trans* as reported in the literature [28,29]. All phosphorus ligand solutions were prepared immediately before each titration by dissolving the appropriate amount of ligand in the desired degassed solvent followed by vigorous stirring.

3.2. ITC experimental procedure for binding phosphorus ligands to $PdCl_2(\text{solvent})_2$

ITC experiments were performed using a NanoITC III calorimeter (TA Instruments, New Castle, DE) equipped with hastelloy cells ($V = 1.056$ mL). All titrations were carried out at 25 °C using a 250- μ L syringe at a stirring rate of 250 rpm. The sample cell contained $PdCl_2(\text{solvent})_2$ and the reference cell contained the chosen solvent. All solvents were degassed prior to titration. The “heat flow” baseline was allowed to equilibrate once the reference and sample solutions were loaded into the cells. The titrations began after equilibration of the power rating. Titrations were run as an incremental series of injections of the appropriate phosphorus ligand into the $PdCl_2(\text{solvent})_2$ solution. Blank experiments were conducted under identical conditions with only solvent in the sample cell to

experimentally determine the heat of mixing of the phosphorus ligands with the pure solvent. These blanks were subtracted from the experiments with $PdCl_2(\text{solvent})_2$ in the cell and integrated to isolate the heat evolved from metal–ligand interactions. Data analysis was performed using NanoAnalyze v2.1 from TA Instruments using the Independent Sites algorithm (see Section 2 for derivations of the appropriate models) [26]. We used a modified version of the Multiple Sites model in Microsoft Excel in order to account for the inability of NanoAnalyze to fit integrated heat data near zero accurately. We used the Solver function in Excel to minimize the sum of the squares of the differences between the measured heat and the calculated heats. The first integrated heat point in each data set is omitted from each fit because the syringe allows for a miniscule amount of ligand to mix before the experiment starts which makes the first data point unreliable. Error analysis was also performed using NanoAnalyze v2.1 via its Statistics function. The uncertainties in the parameters obtained from the fits are calculated by adding perturbations to the optimized fits and then refitting the models for a set number of trials. Each perturbation obeys a Gaussian distribution with the same standard deviation generated from the original fit. The error in each data set was determined within one standard deviation for 1000 trials. The error values reported in the main text for the K values are also multiplied by the factor outside of the parentheses. For example, a K value of $(5.99 \pm 0.01) \times 10^5$ means that the error is 0.01×10^5 , or 1000. Independent verification of K values was unsuccessful due to poor detection of species by UV–Vis and ^{31}P NMR spectroscopies over the most appropriate ranges of concentrations. Specifically, as Hirose details, higher K values require lower concentrations of metal and ligand in order to detect the resulting complexes reliably, and for our systems, we could not detect appreciable signals at the recommended concentrations (less than 1 μ M for metal and ligand for K values in excess of 10^5 M^{-1}) [30].

3.3. ^{31}P NMR characterization of reaction intermediates and products

Mixtures of one or two equivalents of phosphorus ligand to one equivalent of $PdCl_2(\text{solvent})_2$ were prepared in advance and allowed to stir at room temperature for 1 h. An aliquot of the Pd solution was mixed with an equal volume of deuterated solvent (Cambridge Isotope Laboratories) in an NMR tube. Samples were run on a Bruker AV-360 at room temperature with proton decoupling. Each sample was run for 128 scans and each spectrum was observed for the chemical shifts of the Pd complexes.

3.4. Solution calorimetry

Solution calorimetry experiments were performed in a TAM III microcalorimeter (TA Instruments) at 25 °C. Samples of PPh_3 and $P(OPh)_3$ were placed into glass ampoules and sealed with wax to prevent premature mixing of solvent with the ligands. Sealed ampoules were immersed in 25 mL of MeCN in a reaction cell and stirred at 600 rpm. Ampoules were then broken and the ligand (solute) was allowed to mix with the solvent for 1 h while monitoring the heat flow. An electronic heat pulse was applied to the reaction cell before and after dissolution to calibrate the heat capacity in each instance. An empty ampoule (blank) was broken to account for the heat evolved due to breaking the ampoule. The total heat evolved or absorbed during each experiment was obtained using the Analyze Experiment function in the SolCal v1.2 software (TA Instruments). Each heat value was then corrected for the blank experiment and then normalized to the total amount of moles of solute dissolved to calculate the enthalpy of dissolution. The uncertainty for each value originated from the average difference between the evolved heats for multiple experiments.

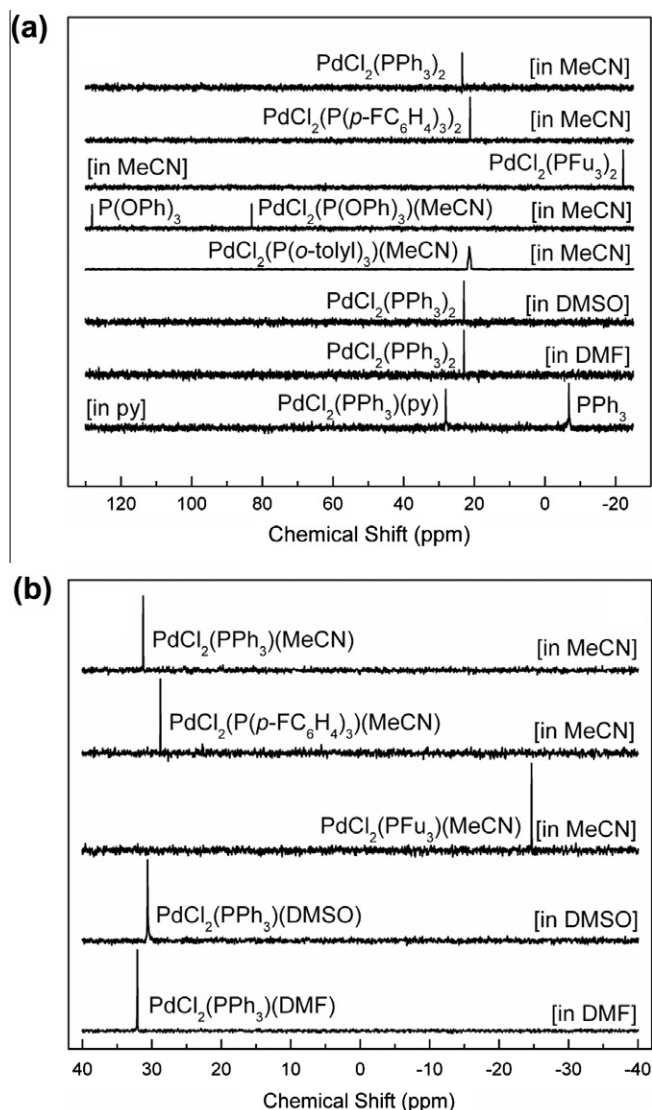


Fig. 1. (a) ^{31}P NMR spectra of $\text{PdCl}_2(\text{solv})_2$ and 2 equivalents of phosphorus ligand as synthesized in the ITC. (b) ^{31}P NMR spectra of $\text{PdCl}_2(\text{solv})_2$ and 1 equivalent of phosphorus ligand for verification of the intermediates is presented in Scheme 1. The resulting Pd–P complexes, along with the reaction solvents, are listed for each spectrum.

4. Results and discussion

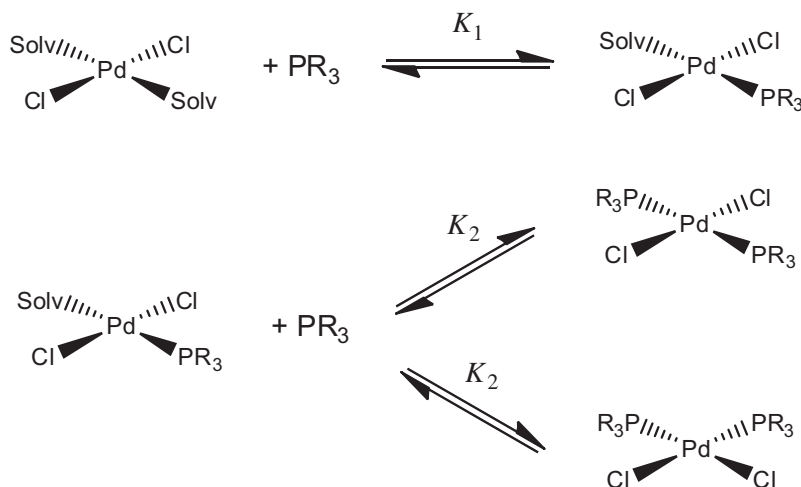
4.1. ^{31}P NMR results for phosphorus ligand binding to $\text{PdCl}_2(\text{solv})_2$

Fig. 1a shows the ^{31}P NMR data for the final bis-ligated complexes and Fig. 1b shows ^{31}P NMR data for the intermediate mono-ligated complexes formed (applicable for the complexes in which no free ligand was observed in the presence of two equivalents of ligand). For two equivalents, $\text{PdCl}_2(\text{PPh}_3)_2$ ($\delta = 23.4$ ppm) and $\text{PdCl}_2(\text{P}(p\text{-FC}_6\text{H}_4)_3)_2$ ($\delta = 21.2$ ppm) exhibited downfield singlets characteristic of the *trans* complex while $\text{PdCl}_2(\text{PFu}_3)_2$ ($\delta = -22.2$ ppm) exhibited the upfield singlet characteristic of the *cis* complex [31,32]. A mixture of $\text{PdCl}_2(\text{MeCN})_2$ and $\text{P}(\text{OPh})_3$ displayed singlets at $\delta = 83.0$ ppm indicative of the complex $\text{PdCl}_2(\text{P}(\text{OPh})_3)(\text{MeCN})$ and at $\delta = 128.2$ ppm indicative of free $\text{P}(\text{OPh})_3$, which agreed with the ITC results. Both $\text{PdCl}_2(\text{PPh}_3)_2$ in DMSO ($\delta = 23.0$ ppm) and DMF ($\delta = 23.0$ ppm) showed singlets characteristic of the *trans* complex. The addition of two equivalents PPh_3 to $\text{PdCl}_2(\text{py})_2$ produced two singlets: one at $\delta = 28.1$ ppm, indicative

of the mono-ligated complex $\text{PdCl}_2(\text{PPh}_3)(\text{py})$, and one at $\delta = -6.8$ ppm, indicative of free PPh_3 . Dissolution of pure $\text{PdCl}_2(\text{PPh}_3)_2$ into *py* yielded an identical spectrum to the solution of $\text{PdCl}_2(\text{py})_2$ and PPh_3 while a solution of pure oxidized triphenylphosphine, OPPh_3 , produced a singlet at $\delta = 24.8$ ppm, leading to the conclusion that only one equivalent of PPh_3 binds to $\text{PdCl}_2(\text{py})_2$ in *py*. A broad resonance was observed for mixtures of $\text{PdCl}_2(\text{MeCN})_2$ and $\text{P}(o\text{-tolyl})_3$ at $\delta = 21.7$ ppm, which is shifted from free $\text{P}(o\text{-tolyl})_3$ at $\delta = -31.6$ ppm. ITC results show that only one equivalent of $\text{P}(o\text{-tolyl})_3$ was able to bind, so we attribute this broad resonance to the existence of $\text{PdCl}_2(\text{P}(o\text{-tolyl})_3)(\text{MeCN})$. No evidence of chloro-bridged Pd dimers or ionization isomers was observed for any of the tested ligands and solvents. For one equivalent of ligand, PPh_3 ($\delta = 31.2$ ppm), $\text{P}(p\text{-FC}_6\text{H}_4)_3$ ($\delta = 28.8$ ppm), and PFu_3 ($\delta = -24.7$ ppm) have different resonances than their respective two equivalent (*cis* or *trans*) complexes. The PPh_3 resonance corresponds to coordinated ligand with a bound MeCN molecule *trans* to it, meaning that the difference in shifts for the one equivalent complexes compared to the two equivalent complexes is due to the coordination of the second ligand as originally reported by Colacot et al. [33]. Based on these ^{31}P NMR results, we present Scheme 1 as a description of the binding equilibria that occur in the ITC experiments. Scheme 1 is a specific representation of Eqs. (3) and (4) and describes both independent (just the K_1 equilibrium reaction) and multiple-site binding. For our systems, we observed one equivalent of bound ligand for the independent cases while we observed two equivalents of bound ligand for the multiple site cases.

4.2. ITC results for binding phosphorus ligands to $\text{PdCl}_2(\text{MeCN})_2$

Fig. 2 shows thermograms for binding ligands to **1** in MeCN at 25 °C and the integrated heats and the best-fit binding models for each system as measured by ITC; best-fit parameters are compiled in Table 2. Note that n_1 and n_2 refer to the step-by-step stoichiometries presented in Eqs. (3) and (4) and the overall binding equilibria presented in Scheme 1 ($n = n_1 + n_2$). Additionally, we provide the ITC experimental conditions in Table A1 of the Supporting Information. The ligands exhibited two binding modes with Pd: either two ligands were able to bind to the same Pd atom, each ligand with its own thermodynamic affinity for the Pd center as expressed in Eqs. (3) and (4), or only one ligand was able to bind to Pd as described by Eq. (3) only (independent binding). The difference in affinities between sites on the same Pd atom is due to the presence of bound phosphorus ligand after the first equilibrium step, which changes the ground-state thermodynamics of the intermediate complex when compared to **1**, resulting in two distinct equilibrium constants for identical ligands (K_1 and K_2) [34]. As seen in Section 4.1, two equivalents of PPh_3 , PFu_3 , and $\text{P}(p\text{-FC}_6\text{H}_4)_3$ were able to bind to **1** in MeCN, while only one equivalent each of $\text{P}(\text{OPh})_3$ and $\text{P}(o\text{-tolyl})_3$ were able to bind. ^{31}P NMR confirmed that PPh_3 and $\text{P}(p\text{-FC}_6\text{H}_4)_3$ formed the *trans* product only while PFu_3 formed the *cis* product only in MeCN (Fig. 1a). Redfield and Nelson studied the thermodynamics of the *cis*–*trans* isomerization of Pd(II)–phosphine complexes and found the *cis* isomer was generally the most stable by as many as two orders of magnitude in K [35]. For the *trans* complexes, this instability is reflected in lower K_2 values, while the more stable *cis* complex has a higher K_2 value. We are not ascribing these differences in K_2 between the *cis* and *trans* complexes to the well-known *trans* influence because both chloride ligands remain bound in the *cis* complex. The *trans* influence is the ability of a ligand already bound to a metal center to weaken the bond of the ligand *trans* to it, altering the ground-state thermodynamics of the complex itself [34]. Empirically, phosphorus ligands are better *trans* directors than Cl ligands, but our ^{31}P NMR data confirm that the Cl ligands are not substituted, so we attribute the formation of both *cis* and *trans* complexes to the



Scheme 1. Illustration of metal–ligand equilibria in solution. For each equilibrated step, a PR_3 ligand displaces a bound solvent molecule (solv). For cases where two equivalents of ligand bind, either the *cis* (PFu_3) or *trans* (PPh_3 and $\text{P}(p\text{-FC}_6\text{H}_4)_3$) product is formed exclusively.

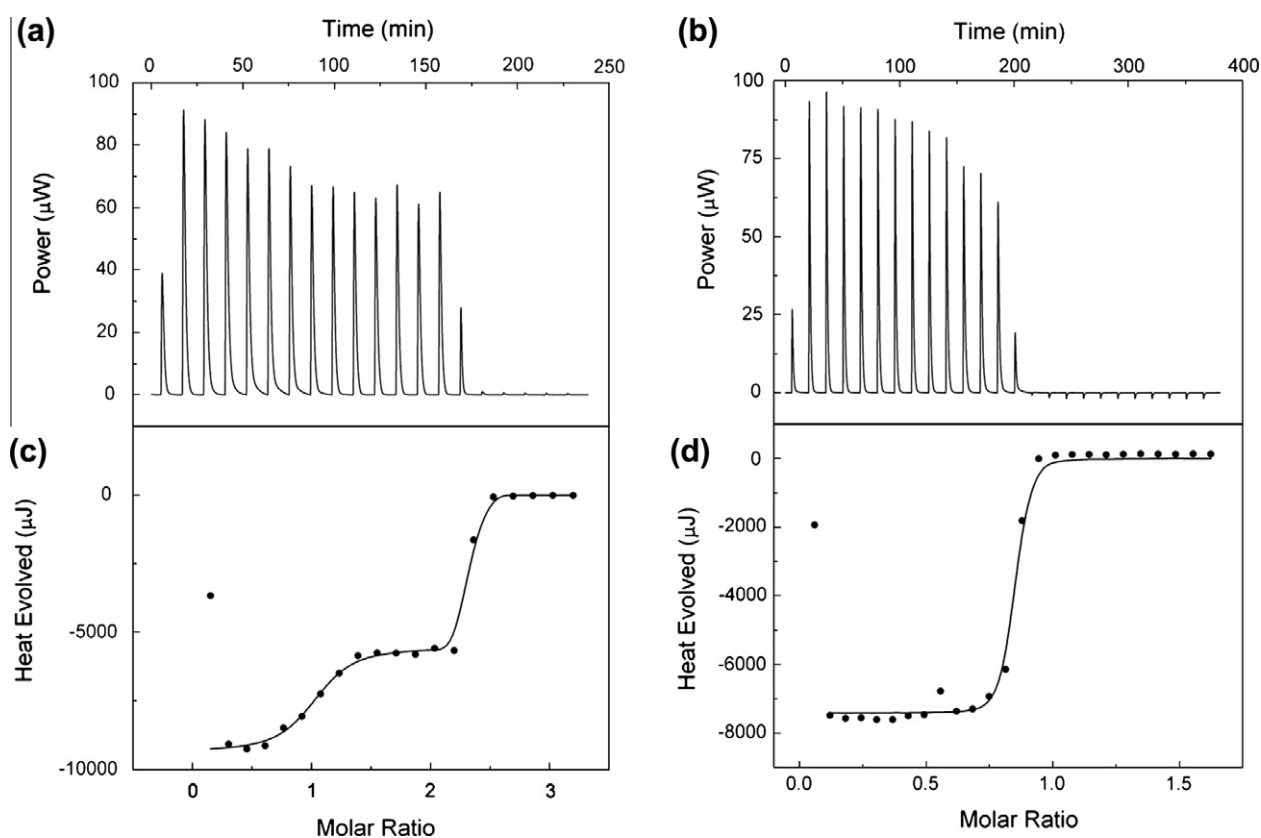


Fig. 2. Real-time ITC thermograms for (a) PPh_3 and (b) P(OPh)_3 binding to **1** in MeCN at 25 °C with (c) and (d) as the respective integrated heat data with fitted models. “Power” refers to the thermal compensation of the calorimeter to keep the sample at a constant temperature (positive peaks are exothermic – the heat evolved reduces the power compensation resulting in a positive value when the baseline is subtracted). See Fig. A1 in the Supporting Information for thermograms of the other ligands.

inherent weakness of the coordinated MeCN molecules. We confirmed metal–ligand binding ratios using UV–Vis spectroscopy and we provide the data in Fig. A3 of the Supporting Information [30]. As discussed in Section 2, the binding sites on the Pd center are thermodynamically independent and the state of one site, bound or unbound, does not affect the affinity of the other site [26]. This trait is reflected in the shapes of the isotherms as two different sigmoidal regions (see Fig. 2a), for the three ligands for which two equivalents of ligand bind, characteristic of multiple-

site binding. Conversely, the two ligands for which only one equivalent binds display a single inflection point, characteristic of independent binding. The different binding modes are consistent with the Tolman cone angles and electronic parameters of phosphites as compared to phosphines. $\text{P}(o\text{-tolyl})_3$ has the largest cone angle, 194°, so it is logical that only one ligand binds to the Pd centers in solution [1]. P(OPh)_3 is the poorest electron donor, though being a triarylphosphite, it is a better π -acceptor than the triarylphosphine, PPh_3 [1,34]. It is also a better π -acceptor than $\text{P}(o\text{-tolyl})_3$

Table 2
Thermodynamic parameters for the binding of PR₃ ligands to **1** in MeCN at 25 °C. Errors were calculated using the statistics function in NanoAnalyze (see Section 3.2).

Ligand	K_1	ΔG_1	ΔH_1	$T\Delta S_1$	n_1
	K_2 (M ⁻¹)	ΔG_2 (kJ/mol) ^a	ΔH_2 (kJ/mol) ^b	$T\Delta S_2$ (kJ/mol)	
PPh ₃	$(1.20 \pm 0.01) \times 10^9$	-51.8 ± 8.6	-62.4 ± 0.2	-10.6 ± 8.6	1.03 ± 0.01
	$(2.13 \pm 0.01) \times 10^7$	-41.8 ± 5.6	-37.0 ± 0.2	4.8 ± 5.6	1.32 ± 0.01
P(<i>p</i> -FC ₆ H ₄) ₃	$(1.06 \pm 0.01) \times 10^8$	-45.8 ± 3.2	-64.1 ± 0.1	-18.3 ± 3.2	1.02 ± 0.01
	$(2.20 \pm 0.01) \times 10^6$	-36.2 ± 8.7	-37.5 ± 0.1	-1.3 ± 8.7	1.34 ± 0.01
PFu ₃	$(2.27 \pm 0.01) \times 10^5$	-30.6 ± 1.4	-36.7 ± 0.5	-6.1 ± 1.5	1.46 ± 0.01
	$(3.15 \pm 0.01) \times 10^7$	-42.8 ± 4.2	-46.2 ± 0.5	-3.4 ± 4.2	1.03 ± 0.01
P(OPh) ₃	$(2.91 \pm 0.01) \times 10^6$	-36.9 ± 10.9	-123.6 ± 1.0	-86.7 ± 11.0	0.82 ± 0.01
P(<i>o</i> -tolyl) ₃	$(2.49 \pm 0.01) \times 10^5$	-30.8 ± 10.5	-49.7 ± 0.2	-19.0 ± 10.5	1.16 ± 0.01

^a The values for ΔG and $T\Delta S$ were calculated from the given K and ΔH values.

^b The integrated heats for each titration were analyzed using either the multiple sites model or the independent model to obtain binding constants (K_i), enthalpies of binding (ΔH_i), and binding stoichiometries (n_i).

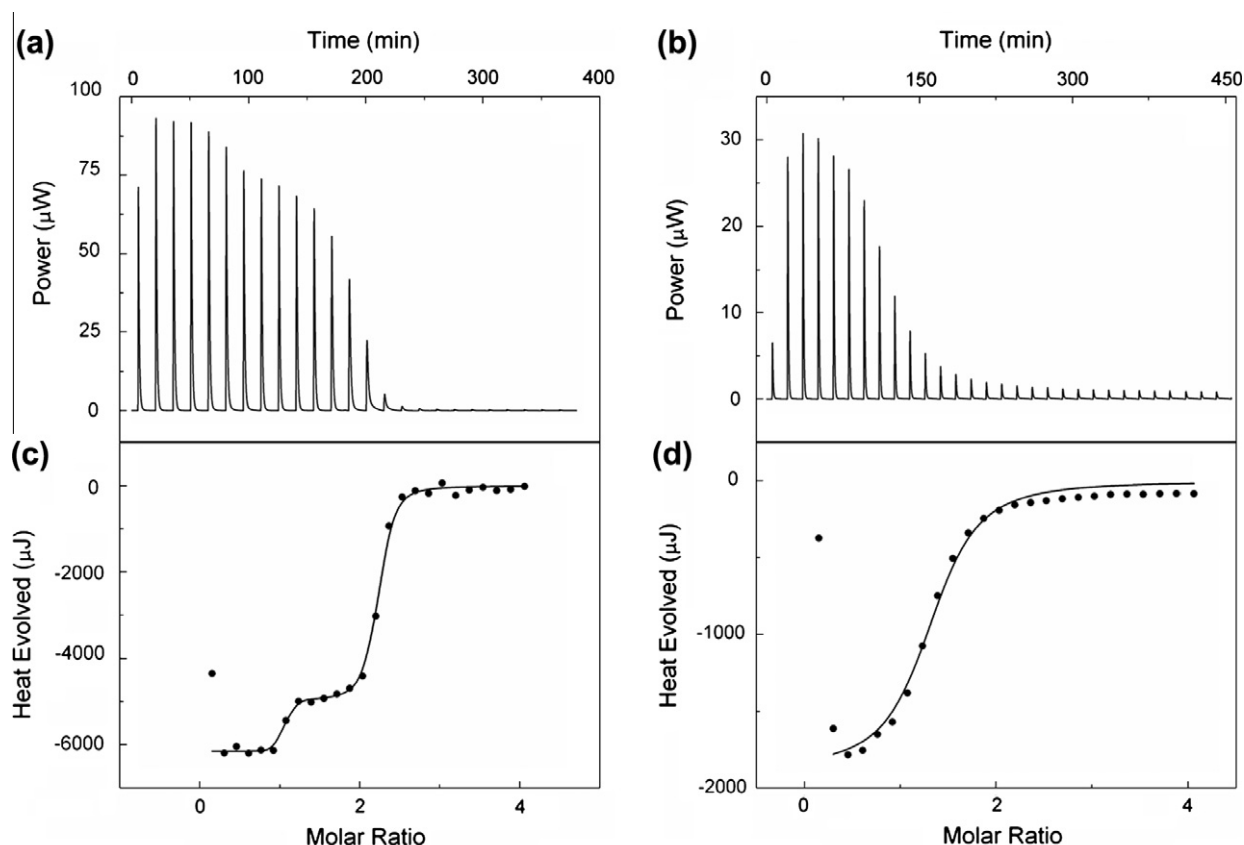


Fig. 3. Real-time ITC thermograms for PPh₃ binding to **2** at 25 °C in (a) DMSO and (b) py with (c) and (d) as the respective integrated heat data with fitted models. See Fig. A2 for the thermogram of DMF.

and has a smaller cone angle, which would explain its larger affinity for binding with **1** [4,36,37]. The Tolman electronic parameter (Table 1) for PPh₃ is less than that of P(*p*-FC₆H₄)₃, indicating that the overall electron-donating ability of PPh₃ is greater [1,34]. These two ligands have identical cone angles and the difference in electron-donating ability explains why PPh₃ binds more strongly to **1**.

4.3. ITC results for binding PPh₃ to PdCl₂(solv)₂

Fig. 3 shows the ITC results for the binding of PPh₃ to **2** in dimethyl sulfoxide (DMSO) and pyridine (py) at 25 °C while the

best-fit parameters for all tested solvents are in Table 3. The structures of **2** are *trans* as reported in the literature and were prepared as reported (see Section 3.1) [28,29]. Multiple-exchanged Pd(DMSO)_{*n*} species (*n* > 1) have been observed, such as [Pd(DMSO)₄]²⁺, but their formation requires silver perchlorate, AgClO₄ (our synthesis does not use silver perchlorate) [38], while our preparation for PdCl₂(py)₂ is identical to that of Gupte and Chaudhari [39] and the formation of PdCl₂(py)₂ was structurally verified via XRD by Liao and Lee [40]. Therefore, we do not expect formation of either Pd(DMSO)_{*n*} or Pd(py)_{*n*} (*n* > 1). For DMSO and *N,N*-dimethylformamide (DMF), two equivalents of ligand bind as

Table 3Thermodynamic properties for the binding of PPh₃ to **2** in various solvents at 25 °C. Errors were calculated using the statistics function in NanoAnalyze (see Section 3.2).

Solvent	K_1 K_2 (M ⁻¹)	ΔG_1 ΔG_2 (kJ/mol)	ΔH_1 ΔH_2 (kJ/mol)	$T\Delta S_1$ $T\Delta S_2$ (kJ/mol)	n_1 n_2
MeCN	$(1.20 \pm 0.01) \times 10^9$ $(2.13 \pm 0.01) \times 10^7$	-51.8 ± 8.6 -41.8 ± 5.6	-62.4 ± 0.2 -37.0 ± 0.2	-10.6 ± 8.6 4.8 ± 5.6	1.03 ± 0.01 1.32 ± 0.01
DMSO	$(2.55 \pm 0.01) \times 10^8$ $(1.75 \pm 0.01) \times 10^5$	-48.0 ± 3.3 -29.9 ± 9.8	-41.0 ± 0.1 -33.2 ± 0.3	6.9 ± 3.3 -3.3 ± 9.8	1.06 ± 0.02 1.17 ± 0.01
DMF	$(2.51 \pm 0.01) \times 10^7$ $(7.64 \pm 0.01) \times 10^4$	-42.2 ± 1.3 -27.9 ± 1.4	-62.8 ± 0.2 -35.5 ± 0.1	-20.5 ± 1.4 -7.7 ± 1.4	0.90 ± 0.01 1.09 ± 0.02
py	$(2.08 \pm 0.01) \times 10^4$	-24.6 ± 7.0	-12.5 ± 0.3	12.1 ± 7.0	1.29 ± 0.02

seen in MeCN. In py, only one ligand binds, which is attributed to two factors. It has a high donor number (*DN*) which is an empirical measure of the ability of a solvent to donate electrons to a solute, PdCl₂ [41]. This evidence indicates that a py molecule (*DN* = 138.5 kJ/mol, *AN* = 14.2 (unitless), see below for definition of *AN*) binds to the Pd center, occupying one of the sites as seen by ITC. The other factor can be traced to a calorimetric study of the thermodynamics of ligand exchange for PdCl₂(C₇H₅N)₂ to determine relative displacement energies (RDEs) comparing the intrinsic binding strength of one ligand to another, which found that py has an RDE less than that of PPh₃, which means that displacing PPh₃ has a more unfavorable contribution to ΔG [42]. We tested py binding to **1** in MeCN using ITC and found that only one equivalent of py binds (shown in our other study [43]), agreeing with the RDE study. For our system, PdCl₂(py)₂ is in excess py, whereas the previous study was conducted in dichloromethane, so it is reasonable to attribute the presence of only one bound PPh₃ ligand to the excess of py relative to unbound PPh₃ (Fig. 3). The binding is strongest in MeCN (highest *K* values) and weakest in DMF (lowest *K* values). In terms of *DN* and acceptor number (*AN*, which is an empirical measure of the ability of a solvent to accept electrons from solutes), MeCN (*DN* = 59.0 kJ/mol, *AN* = 18.9) is the weakest electron donor and a better electron acceptor than DMF (*DN* = 111.3 kJ/mol, *AN* = 16.0), so bound MeCN molecules are more easily displaced by free PPh₃ [41]. The best-fit values of binding in DMSO (*DN* = 124.7 kJ/mol, *AN* = 19.3) and DMF are similar in terms of the orders of magnitude of the obtained *K* values due to having similar *DN* and *AN* values (note: all *DN* and *AN* values are taken from Refs. [41,44]).

4.4. Understanding the contributions to the enthalpy and entropy of binding

The obtained ΔH and ΔS values provide insight as to what the dominant effects are for a given set of metal–ligand interactions. The obtained ITC parameters are observed values, rather than intrinsic values. The observed enthalpy includes the loss of solute–solvent bonds in the form of solvent reorganization (PdCl₂ and ligand are solutes), the loss of van der Waals forces, solvation and conformational changes at the binding site, and metal–ligand binding [45,46]. The observed entropy change includes contributions from losses of translational, rotational, and vibrational degrees of freedom and from the solvation and desolvation of the solutes; however, the main positive contribution to the observed entropy is expulsion of solvent molecules bound to the metal, which normally manifests itself as an increase in entropy [45,46]. From Table 2, ligand binding is enthalpy-driven because of the large, exothermic enthalpies and small entropies. The ligands for which two equivalents bind to **1** all have an increase in entropy after the first ligand is bound, which is attributed primarily to

the displacement of the last bound solvent molecule. It is noteworthy that py has nearly equal enthalpy and entropy contributions. Regarding the large RDE of py, it makes sense that the observed ΔH decreased in magnitude relative to the other solvents because the displacement of the bound py contributes unfavorably to ΔG [42,47]. For MeCN and DMF, the entropic contributions increase after the second ligand binds, in agreement with the trend from the different ligands. The DMSO system decreases in entropy after the second ligand binds because it has the highest *AN* of the tested solvents; it is the best electron acceptor and the desolvation of the PPh₃ ligand, which has a lone pair of electrons on the P atom, is not as favorable as it is in the other solvents. Our ΔS_2 values, except for the DMSO system, are all smaller in magnitude than their respective ΔS_1 values because of fluxionality at the Pd centers (with respect to solvent molecules). Certainly, we expect the Pd–P complexes to be fluxional in their own right, but the PdCl₂(solvent)₂ complexes rapidly exchange bound solvent molecules as ligands with bulk solvent molecules. As ligands bind to the Pd center, this solvent fluxionality is lost, which manifests itself as a decrease in entropy. We presume this loss in fluxionality to be less dramatic for mono-ligated Pd–P complexes than for PdCl₂(solvent)₂, which explains why ΔS_2 values are smaller in magnitude than ΔS_1 values. Solvent molecules can form adducts with the ligands, which would change their overall polarity and subsequently change the enthalpy of solvation of the products (Pd–P complexes). Partenheimer et al. studied this effect for acid–base systems in cyclohexane and CCl₄ and noticed more cyclohexane molecules formed adducts with the base, dimethylacetamide, than did CCl₄ which explained the differences in the observed enthalpies of acid–base reactions between the solvents [48]. Overall, ligand binding is enthalpy-driven, that is, the large enthalpy values indicate that solvent reorganization contributes greatly to the observed enthalpies, as originally noted by Chervenak and Toone [49]. Solvent reorganization includes the loss of solute–solvent interactions (in the solvation shells around the solutes) during the binding event that is necessarily accompanied by new solvent–solvent interactions that occur once the expelled solvent molecules reenter the bulk [50]. In their study, Chervenak and Toone used ITC to measure the binding thermodynamics of several systems, such as protein–carbohydrate and protein–peptide binding equilibria, in both H₂O and D₂O and determined that decreased ΔH values in D₂O were compensated by changes in ΔS , practically leaving ΔG constant. They assumed that intrinsic ligand–receptor binding was invariant of the nature of the solvent, meaning that solvent reorganization accounted for 25–100% of the observed binding enthalpies for the systems studied [49].

Examination of theoretical Pd–P binding energies helps to explain how the observed binding enthalpies differ greatly from one P ligand to another in solution. Fey et al. determined bond dissociation energies (BDEs) from [PdCl₃L][−] where L represents a

specific P ligand [51]. For the five P ligands in our study, the BDEs range from ~108 to 148 kJ/mol, so it is unsurprising to learn that ligand binding is enthalpy-driven from a theoretical perspective. Their calculations do not account for the effect of solvent and their model Pd structures are obviously different from ours, but these values are a reasonable estimate for theoretical Pd–P binding energies. With the exception of P(OPh)₃, our observed enthalpies are a factor of 2–3 smaller for binding one equivalent of ligand to Pd, which we attribute to the fact that the ligands and Pd complexes are solvated. Additionally, their model Pd compound is negatively charged, while ours is neutral.

The drastic variation in thermodynamic values obtained for P(OPh)₃ relative to the other P ligands warrants further discussion. The other ligands in this study have rigid aryl groups connected directly to the P atom, whereas the phenyl groups in P(OPh)₃ are linked to the P atom by O atoms, which allows for more rotational freedom when the ligand is unbound. All ligands will lose translational and rigid-body rotational entropy upon binding, but P(OPh)₃ would seem to suffer the largest penalty. The enthalpies of dissolution for both ligands, PPh₃ (26.21 ± 0.04 kJ/mol) and P(OPh)₃ (6.86 ± 0.01 kJ/mol), are endothermic. In both cases, there are intermolecular forces that must be overcome in order for dissolution to occur. The enthalpy of solution for PPh₃ is larger in magnitude because its lattice energy must be overcome in order for it to dissolve (it is a solid) while P(OPh)₃ is a liquid and has no such energy. If the enthalpy of fusion for PPh₃ (19.69 kJ/mol) [52] is taken into account as a crude approximation of its lattice energy, then dissolution of a hypothetical PPh₃ liquid would be the difference between the enthalpy of dissolution and the enthalpy of fusion, which is 6.52 kJ/mol, slightly smaller in magnitude than the enthalpy of solution of P(OPh)₃, which is 6.86 kJ/mol. Since the enthalpy of dissolution for P(OPh)₃ is positive, overcoming its own intermolecular forces and breaking up solvent–solvent intermolecular forces are larger in combined magnitude than solute–solvent interactions. The inability of P(OPh)₃ to overcome these forces which, along with its enormous rotational entropy penalty, explains why P(OPh)₃ has such a large, negative entropy of binding [53]. Searle and Williams estimate an entropy loss of 8.8–44.8 kJ/mol (for $T\Delta S$) at 25 °C for the binding of small molecules to proteins in solution due to lost rigid-body entropy, noting that the larger losses in entropy are associated with larger increases in enthalpy, that is, enthalpy–entropy compensation [54]. The desolvation of the π -acidic P(OPh)₃ upon binding would decrease entropy due to the nature of MeCN being a good electron acceptor.

5. Conclusions

We have provided detailed analysis of the thermodynamics of the binding of P ligands to **1** and the effect of different solvents on the thermodynamics of binding to PPh₃ to **2**. We observed via ³¹P NMR spectroscopy that one or two equivalents of ligand bind to the Pd centers. For bulkier ligands and poor electron-donating ligands, only a single ligand was able to bind to **1**. Our ITC experiments demonstrated that ligands interact with the Pd center in two binding modes: either two equivalents of ligands bind to sites of different affinity on the same Pd center or only one equivalent of ligand binds. For the bis-ligated complexes, the addition of the second ligand proved to be more stable when forming a *cis* complex when compared to the *trans* complexes. The electronic influences of the different solvents also affected the binding ability of PPh₃. MeCN was the most easily displaced due to its weak-coordinating ability coupled with its strong electron-accepting ability. The strong electron-donating ability and RDE of py restricted binding to a single PPh₃ ligand while two equivalents of PPh₃ were able to bind in the other three solvents (MeCN, DMSO, and DMF).

We found that these metal–ligand interactions are enthalpy-driven. These large, exothermic enthalpies indicate that solvent reorganization likely contributed greatly to the observed enthalpies and played an active role in the metal–ligand equilibria. We attributed the ability of the solvent molecules to interact with the solutes as another contributor to the observed enthalpies of binding. All ligands for which two equivalents bind to **1** had an increase in entropy after the second ligand was bound, likely due to displacement of a bound solvent molecule. The largest decrease in observed entropy was seen for P(OPh)₃ and was attributed to a loss of translational and rigid-body rotational entropies.

Acknowledgments

The work was supported by The Pennsylvania State University and The Penn State Institutes of Energy and Environment (PSIEE) through start-up funds provided to RMR and a 3M Non-Tenured Faculty Grant. K.G. acknowledges support from the NASA WISER program for undergraduate research.

Appendix A. Supplementary material

Supplementary data associated with this article can be found, in the online version, at <http://dx.doi.org/10.1016/j.jcat.2013.02.020>.

References

- [1] C.A. Tolman, Chem. Rev. 77 (1977) 313–348.
- [2] R.S. Drago, Coord. Chem. Rev. 33 (1980) 251–277.
- [3] O. Kuhl, Coord. Chem. Rev. 249 (2005) 693–704.
- [4] M.R. Wilson, D.C. Woska, A. Prock, W.P. Giering, Organometallics 12 (1993) 1742–1752.
- [5] G.C. Vogel, R.S. Drago, J. Chem. Educ. 73 (1996) 701–707.
- [6] V.M. Nosova, Y.A. Ustynyuk, L.G. Bruk, O.N. Temkin, A.V. Kisin, P.A. Storozhenko, Inorg. Chem. 50 (2011) 9300–9310.
- [7] J.A. Osborn, F.H. Jardine, J.F. Young, G. Wilkinson, J. Chem. Soc. A (1966) 1711–1732.
- [8] R.F. Heck, J.P. Nolley Jr., J. Org. Chem. 37 (1972) 2320–2322.
- [9] A. Suzuki, J. Organomet. Chem. 576 (1999) 147–168.
- [10] K. Sonogashira, Y. Tohda, N. Hagihara, Tetrahedron Lett. (1975) 4467–4470.
- [11] R. Jira, Angew. Chem. Int. Ed. 48 (2009) 9034–9037.
- [12] J.A. Keith, P.M. Henry, Angew. Chem. Int. Ed. 48 (2009) 9038–9049.
- [13] K.S. Yoo, C.H. Yoon, K.W. Jung, J. Am. Chem. Soc. 128 (2006) 16384–16393.
- [14] C. Martinez, R. Alvarez, J.M. Aurrecochea, Org. Lett. 11 (2009) 1083–1086.
- [15] T.J. Marks, M.R. Gagne, S.P. Nolan, L.E. Schock, A.M. Seyam, D. Stern, Pure Appl. Chem. 61 (1989) 1665–1672.
- [16] T. Wiseman, S. Williston, J.F. Brandts, L.N. Lin, Anal. Biochem. 179 (1989) 131–137.
- [17] E. Freire, O.L. Mayorga, M. Straume, Anal. Chem. 62 (1990) A950–A959.
- [18] M.J. Cliff, J.E. Ladbury, J. Mol. Recogn. 16 (2003) 383–391.
- [19] M.J. Cliff, A. Gutierrez, J.E. Ladbury, J. Mol. Recogn. 17 (2004) 513–523.
- [20] A. Ababou, J.E. Ladbury, J. Mol. Recogn. 19 (2006) 79–89.
- [21] A. Ababou, J.E. Ladbury, J. Mol. Recogn. 20 (2007) 4–14.
- [22] O. Okhrimenko, M. Jelesarov, J. Mol. Recogn. 21 (2008) 1–19.
- [23] S. Bjelic, I. Jelesarov, J. Mol. Recogn. 21 (2008) 289–311.
- [24] R.J. Falconer, A. Penkova, I. Jelesarov, B.M. Collins, J. Mol. Recogn. 23 (2010) 395–413.
- [25] R.J. Falconer, B.M. Collins, J. Mol. Recogn. 24 (2010) 1–16.
- [26] E. Freire, A. Schon, A. Velazquez-Campoy, in: M.L. Johnson, J.M. Holt, G.K. Ackers (Eds.), Methods in Enzymology: Biothermodynamics, vol. 455, Part A, Elsevier Academic Press Inc., San Diego, 2009, pp. 127–155.
- [27] G.M.K. Poon, Anal. Biochem. 400 (2010) 229–236.
- [28] B.B. Wayland, R.F. Schramm, Inorg. Chem. 8 (1969) 971–976.
- [29] K. Nakamoto, Infrared and Raman Spectra of Inorganic and Coordination Compounds, Wiley-Blackwell, distributor, Hoboken, NJ, 2009.
- [30] K. Hirose, J. Inclusion Phenom. Macrocyclic Chem. 39 (2001) 193–209.
- [31] S.O. Grim, R.L. Keiter, Inorg. Chim. Acta 4 (1970) 56–60.
- [32] C.M. Hettrick, W.J. Scott, J. Am. Chem. Soc. 113 (1991) 4903–4910.
- [33] T.J. Colacot, W.A. Carole, B.A. Neide, A. Harad, Organometallics 27 (2008) 5605–5611.
- [34] R.H. Crabtree, The Organometallic Chemistry of the Transition Metals, Wiley, Hoboken, NJ, 2009, xiii, 505p.
- [35] D.A. Redfield, J.H. Nelson, Inorg. Chem. 12 (1973) 15–19.
- [36] A.L. Fernandez, C. Reyes, A. Prock, W.P. Giering, Perkin 2 (2000) 1033–1041.
- [37] A.L. Fernandez, M.R. Wilson, A. Prock, W.P. Giering, Organometallics 20 (2001) 3429–3435.
- [38] B.B. Wayland, R.F. Schramm, Chem. Commun. (1968) 1465–1466.
- [39] S.P. Gupte, R.V. Chaudhari, J. Mol. Catal. 24 (1984) 197–210.

- [40] C.Y. Liao, H.M. Lee, *Acta Crystallogr. Sec. E: Struct. Rep. Online* E62 (2006) m680–m681.
- [41] Y. Marcus, *J. Solution Chem.* 13 (1984) 599–624.
- [42] W. Partenheimer, E.F. Hoy, *Inorg. Chem.* 12 (1973) 2805–2809.
- [43] E.G. Moschetta, K.M. Gans, R.M. Rioux, Personal communication.
- [44] R.W. Taft, N.J. Pienta, M.J. Kamlet, E.M. Arnett, *J. Org. Chem.* 46 (1981) 661–667.
- [45] I. Jelesarov, H.R. Bosshard, *J. Mol. Recogn.* 12 (1999) 3–18.
- [46] A. Bronowska, in: J.C. Moreno-Pirajan (Ed.), *Thermodynamics – Interaction Studies – Solids, Liquids, and Gases*, InTech, 2011.
- [47] W. Partenheimer, B. Durham, *J. Am. Chem. Soc.* 96 (1974) 3800–3805.
- [48] W. Partenheimer, T.D. Epley, R.S. Drago, *J. Am. Chem. Soc.* 90 (1968) 3886–3888.
- [49] M.C. Chervenak, E.J. Toone, *J. Am. Chem. Soc.* 116 (1994) 10533–10539.
- [50] E. Grunwald, C. Steel, *J. Am. Chem. Soc.* 117 (1995) 5687–5692.
- [51] N. Fey, B.M. Ridgway, J. Jover, C.L. McMullin, J.N. Harvey, *Dalton Trans.* 40 (2011) 11184–11191.
- [52] D.R. Kirklin, E.S. Domalski, *J. Chem. Thermodyn.* 20 (1988) 743–754.
- [53] C.W. Murray, M.L. Verdonk, *J. Comput.-Aided Mol. Des.* 16 (2002) 741–753.
- [54] M.S. Searle, D.H. Williams, *J. Am. Chem. Soc.* 114 (1992) 10690–10697.